Int. J. Heat Mass Transfer. Vol. 19, pp. 915–923. Pergamon Press 1976. Printed in Great Britain

PREDICTIONS OF VIGOROUS IGNITION DYNAMICS FOR A PACKED BED OF SOLID PROPELLANT GRAINS

HERMAN KRIER and S. S. GOKHALE
Aeronautical and Astronautical Engineering Department, University of Illinois at Urbana—Champaign, Urbana, IL 61801, U.S.A.

(*Received* 9 *December* 1975)

Abstract—This work represents the key results of a research project to predict the pressure wave propagation and flame spreading in a porous propellant charge ignited at one end by a high explosive initiator. The predictions attempted to model controlled laboratory tests with large grain M30 propellant confined in a cylinder and ignited by detonating an explosive disc at the open end. It was predicted that the magnitude of the initiator mass discharge rate determines the convective flame front speed and the pressure wave propagating into the propellant bed.

NOMENCLATURE

C_v, C_p, specific heat [J/Kg °K];
D_p, particle diameter [mm];
$\mathscr{D}$, drag interaction term [N/m^3];
E, total energy [J/kg];
E_{chem}, total propellant energy release [J/kg];
G_{12}, modified Nusselt number (heat-transfer coefficient) [1/s];
k, thermal conductivity [W/cm K°];
K_m, effective continua parameter;
l_p, length of primer [m];
M, mass of detonator discharge [kg];
n, burning rate index;
P, Pressure [N/m^2];
$\dot{r}$, propellant regression rate, $= bP^n$ [cm/s];
T, temperature [°K];
t, time [s];
t_{dr}, disc rupture time [s];
t_p, igniter action time [s];
U, velocity;
V_F, flame front velocity [mm/μs];
x, coordinate along propellant bed.

Greek symbols

Γ, mass source term, $= 6[(1-\phi)\rho_p\dot{r}]/D_p$ [kg/s·m^3];
ρ, density [kg/m^3];
ϕ, void fraction $= \dfrac{\text{gas volume}}{\text{total volume}}$;
ψ, primer mass discharge per unit length [kg/m·s].

Subscripts

g, gas phase;
p, particle phase;
m, mixture;
0, initial;
12, from solid to gas (21 = from gas to solid).

INTRODUCTION

THIS paper summarizes the research efforts to predict the pressure wave propagation and energy release rate in a prorous solid propellant charge ignited at one end by a detonating initiator. A two-phase reactive code developed previously (see [1–3]) was utilized to predict pressure, density, propellant grain, and temperature distributions during the ignition and flame-spreading sequence. The physical problem may be described as a solid propellant combustion process which is sustained by convection of heat into the unignited propellant. In this application the propellant grains are small and perforated and contained in a thick wall cylindrical chamber which is completely filled. At the open end of the chamber an igniter pellet is detonated, driving high pressure gases into the charge.

The experiments

Ignition transient experiments have been carried out by Knapton, Comer, and Stobie at the Interior Ballistic Laboratory, Ballistic Research Laboratories, APG, Md. in which a bed of M-30, MP triple base propellant confined in a fairly long tube was vigorously ignited at the open end by detonating a tetryl pellet [4]. Figure 1 presents a schematic of the test configuration used at IBL, indicating the location of the initiator and location of four pressure transducers used to monitor the pressure waves during the ignition and flamespreading. A burst disc was located at the closed end in order to terminate the test when the bursting pressure of 14×10^6 N/m^2 was reached at that point. A typical loading density resulted in a porosity of $\phi = 0.47$. The mass of the detonator was 38.2 g. Details of the experiments, data acquisition, and a summary of the results are presented in [4].

The model

The theoretical model applied to describe the ignition transient, pressure wave propagation, and the con-

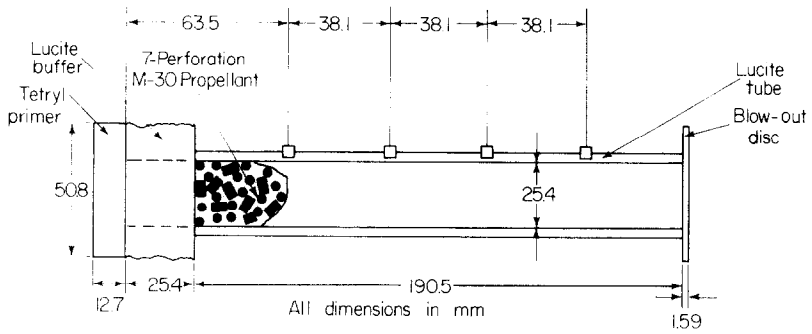

FIG. 1. Schematic of vigorous end-on ignition experiment [4].

vective flame front has been developed and studied in [1–3]. The report by Krier and Gokhale [5] presents additional detailed discussions concerning the application of this particular model to the problem of vigorous ignition of a bed of gun propellant.

The model and assumptions

In general, studies of the dynamics of multiphase systems have the two approaches: (1) Treating the dynamics of single particles and then trying to extend to a multiple particle system in an analogous manner as in molecular theory, or (2) Modifying continuum mechanics of single phase fluid in such a way as to account for the presence of particles.

The extension of multiple particle system from dynamics of single particles has not been particularly successful except in isolated cases. In the continuum mechanics approach the gas and solid are considered as separate continua that interact with each other.

The model used in this study, is based upon the following assumptions [1–3]: (a) the reactions and transfers are exchanges rather than creation or destruction, (b) the motion of mixture is governed by the same equations as is a single body, (c) all species are present simultaneously at all points in space, (d) each species may be considered isolated from the mixture when its motion is calculated, provided that the interaction between the various species are appropriately accounted for, (e) the mixture is a homogeneous substance and obeys the conservation equations governing a single component Newtonian fluid, and (f) the mixture pressure is the sum of species partial pressure.

A discussion of the consequence of these assumptions as they effect the governing conservation equations are presented in [3]. Using these assumptions, the one-dimensional equations (which are derived in detail in [1–2]) are:

Mass balances

Gas phase

$$\frac{\partial}{\partial t}(\phi\rho_g)+\frac{\partial}{\partial x}(\phi\rho_g U_g)=\Gamma_g. \tag{1}$$

Solid phase

$$\frac{\partial}{\partial t}[(1-\phi)\rho_p]+\frac{\partial}{\partial x}[(1-\phi)\rho_p U_p]=\Gamma_p. \tag{2}$$

Momentum balances

Gas phase

$$\rho_g\phi\frac{DU_g}{Dt_g}=\frac{\partial}{\partial x}(\phi p_g)+\frac{\partial}{\partial x}[(U_g-U_m)^2\rho_g\phi]-(U_g-U_m)\Gamma_g+\mathscr{F}. \tag{3}*$$

Solid phase

$$(1-\phi)\rho_p\frac{DU_p}{Dt_p}=\frac{\partial}{\partial x}[(1-\phi)\rho_p(U_p-U_m)^2]-(U_p-U_m)\Gamma_p-\mathscr{F}\frac{(1-\phi)}{\phi}. \tag{4}*$$

Energy balances

Gas phase

$$\begin{aligned}\phi\rho_g\frac{DE_g}{Dt_g}=&\frac{\partial}{\partial x}\{U_g[-\phi P_g+\rho_g\phi(U_g-U_m)^2]\}\\&+\Gamma_g(E^g_{\text{Chem}}-E_g)+\frac{\partial}{\partial x}[\phi\rho_g(U_g-U_m)E_g]\\&-\frac{\partial}{\partial x}\{(U_g-U_m)[-\phi P_g+\phi\rho_g(U_g-U_m)^2]\}\\&+C_g\phi G_{12}(T_p-T_g)\rho_g.\end{aligned} \tag{5}$$

Solid phase

$$\begin{aligned}(1-\phi)\rho_p\frac{DE_p}{Dt_p}=&\frac{\partial}{\partial x}\{U_p[(1-\phi)\rho_p(U_p-U_m)^2]\}\\&+\Gamma_p(E^p_{\text{Chem}}-E_p)\\&+\frac{\partial}{\partial x}[(1-\phi)\rho_p(U_p-U_m)E_p]\\&-\frac{\partial}{\partial x}\{(U_p-U_m)[(1-\phi)\rho_p(U_p-U_m)^2]\}\\&+C_p(1-\phi)\rho_p G_{21}(T_g-T_p).\end{aligned} \tag{6}$$

The auxiliary relations needed are

$$P_g=\rho_g\bar{R}_g T_g \tag{7}$$

and

$$P_p=0 \tag{8}$$

$$\rho_p=\text{constant} \tag{9}$$

$$E_g=C_{v_g}(T_g-T_0)+\tfrac{1}{2}U_g^2 \tag{10}$$

* $\dfrac{D}{Dt_g}=\dfrac{\partial}{\partial t}+U_g\dfrac{\partial}{\partial x}$; $\dfrac{D}{Dt_p}=\dfrac{\partial}{\partial t}+U_p\dfrac{\partial}{\partial x}$.

$$E_p = C_{v_p}(T_p - T_0) + \tfrac{1}{2}U_p^2 \tag{11}$$

$$\rho_m = \rho_{\text{gas}} + \rho_{\text{solid}} \tag{12}$$

or

$$\rho_m = \phi\rho_g + (1-\phi)\rho_p \tag{13}$$

and

$$\rho_m U_m = \phi\rho_g U_g + (1-\phi)\rho_p U_p. \tag{14}$$

The drag (viscous gas–particle) interaction in the momenta balances and the heat-transfer coefficient (the terms noted as G in the energy balances) are inputs to the model, usually taken from correlations of steady-state flow although inert packed beds [6]. Those functions used have been discussed in [2, 3]. In addition the propellant, once ignited, provides hot gases at a rate dependent upon the pressure [2].

For ignition the model assumes that during the unsteady flow process the bulk solid phase temperature, T_p must reach a critical ignition temperature, usually assumed to be at least 20–25 °C above the ambiant initial propellant temperature. Details of the numerical integration scheme used to solve this model are also presented in [3].

The program output gives the values of all the variables over the entire bed at specified time intervals throughout the ignition sequence. Also the location of the flame front is recorded as the bed is ignited.

A typical computer output page as printed is included in the Appendix.

Limitations of model

The concept of continuum mechanics when applied to the case of particulate suspension must be properly qualified by examining the nature of the fluid flow around the particles. In the absence of shear motion, body force, and chemical reaction conservation of momentum of one species of solid particles would be

$$\rho_g \frac{dU_{gi}}{dt} + \rho_p \frac{dU_{pi}}{dt} = -\frac{\partial P}{\partial x_i}. \tag{15}$$

The above relation is true for identical solid particles and if we have "slow" relative motion or "high" concentration of solid particles. Also, equation (15) treats particle phase as a true continuum, that is, not only the gas imparts its momentum to the particles but the cloud of solid particles can transfer its momentum to the gas. This is not always true. But to account for all situations, equation (15) should be modified as

$$\rho_g \frac{dU_{gi}}{dt} + K_m \rho_p \frac{dU_{pi}}{dt} = -\frac{\partial P}{\partial x_i} \tag{16}$$

where $K_m = 1$ when solid particles are accelerated by gas; $K_m < 1$ when solid particles are decelerated by the gas.

Another limit of continuum approximation is that the thermal state of a particle is identified by its temperature. Addition of heat to a moving particle increases the body temperature of the particle, while its velocity arises primarily from particle–fluid interaction [6].

Also with the qualified continuum approximation, the duality of stream lines of particle and fluid must be recognized. Further generalization includes multiplicity of stream lines due to distribution in sizes of particles of various material and charges, etc. [7].

The model assumes one dimensionality. Allowing the fact that the tube diameter is small as compared to the length of the tube, it does not tell anything about the proportion of energy and momentum transfer in the radial direction with the axial direction. Thus, the simulation of three dimensional experiments to one dimensional analytical model needs some kind of correction factor about which very little is known. That is, some kind of scaling relations need to be devised.

The ignition source is essentially modelled as a very short region (planar approximation) in which a known mass is discharged for a prescribed time period. That is, for the one-dimensional analysis the "primer" is assumed to be a source of heat and mass distributed over the first few grid points of the bed length. The hot gases provided by the primer are assumed to be identical to the other gases present.

PREDICTED RESULTS

The model in this study was utilized to predict the pressure wave propagation, flamespreading rate and the subsequent gas dynamics in a bed of multi-perforated gun propellant confined in a tube 25.4 mm in diameter and 191 mm long which is ignited by a short duration large magnitude blast. The results that are presented are therefore for cases of large mass discharge rates inputted at one end of the tube. The overriding questions were: (i) what amount of mass of the tetryl blast actually entered the bed, (ii) how rapidly was this mass discharged, and (iii) over what length was this discharge distributed?

This dilemma was inherent because with such a vigorous ignition source there was no diagnostic test procedure to provide that information. Therefore, we have *a priori* assumed that in the 200-mm long bed of propellant the igniter mass is liberated only in the first 12 mm. We have attempted a few cases in which this length was only 6 mm, but for the large discharge rates required, the results were no longer numerically stable due to the extreme pressure and density gradients predicted. The igniter mass discharge rate, ψ, was calculated such that

$$\psi = \frac{M}{l_p \cdot t_p} \tag{17}$$

where M is the mass of igniter material which has entered the bed, l_p is the distributed length of gas liberation arbitrarily fixed at 12 mm, and t_p is the action (on) time which was typically set to 100 μs.

Figure 2 presents the predictions of the pressure history at four locations in representing the position in the bed where the pressure was recorded in the experiments. The mass discharge rate of $\psi = 3 \times 10^4$ kg/s m^{-1} dumps the entire exploded pellet mass of 38.2 g in form of a hot igniter gas in the 12 mm length for a period of 100 μs. The igniter action time of 100 μs was suggested to represent the detonation of the tetryl initiator, but, of course, the exact time is really not known and

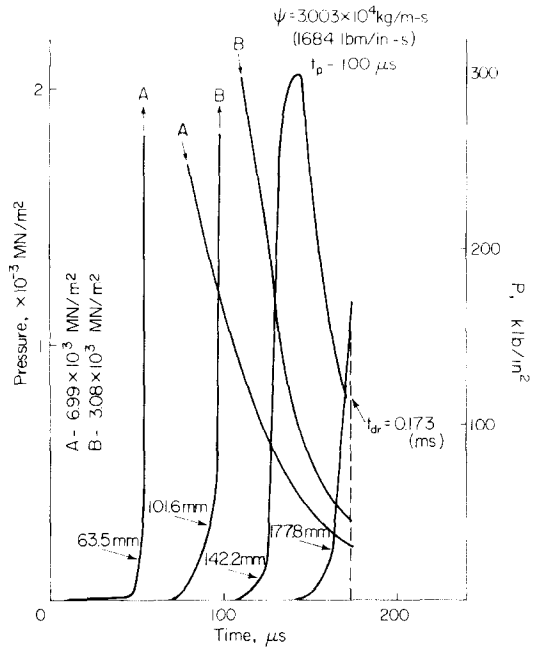

FIG. 2. Predicted pressure history at the four gage locations, assuming total mass discharge of the tetryl initiator.

may even be an order of magnitude lower. The disc is predicted to rupture at 173 μs.

The results shown in Fig. 2, before disc rupture, are totally out of bounds with the experimental results of [4] where the maximum pressure at any of the four gages never exceeded 310 MPa (45 000 psia). Such extreme pressures as 7000 MPa (10^6 psia) are greater by an order of magnitude, and in the theoretical model one must reduce the igniter source strength or the total mass entering the propellant bed.

Figure 3 presents the predictions of the *peak* pressure at all points in the bed for three different assumed values of the igniter mass, all liberated uniformly over 12 mm within the disc rupture time. Any point on these lines might represent a different time; the results shown

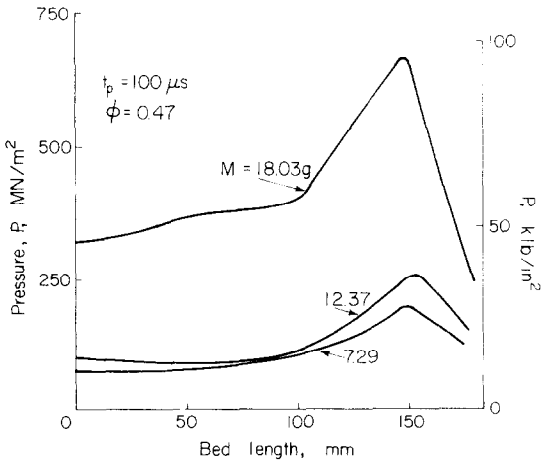

FIG. 3. Predicted peak pressure distribution for three different initiator masses.

in Fig. 3 represent those peak pressures until the disc rupture pressure was reached at the far end. Table 1 lists the inputted parameters used in the model for predictions of the results shown in Figs. 2–12. Such pressures as 700 MPa (95 000 lb/in^2) still rule out a mass of 18 g (ψ = 15 g/mm ms^{-1}). Therefore, if our representation of the spacial distribution of igniter liberation is approximately correct and we are to match the experimental results, then the results shown in Fig. 3 imply that typically only a fraction of the mass of the detonator material enters the tube before disc rupture.

Table 1. Input parameters for University of Illinois Code

Parameter	Value
Propellant	M30 Triple base (7 perforations)
Outer diameter	7.01 mm
Web	1.32 mm
Length	15.85 mm
Density	1.66 g/cm^3
Chemical energy released in burning	1.32×10^2 kcal/kg
Molecular weight of propellant gas	23.2 $\mathrm{lb_m}$/mole
Polytropic gas constant	1.23
Burning rate law	$\dot{r} = b_2 P^n$
b_2	3.60×10^{-7} cm/s(N/m^2)^n
n	0.667
Initial bed porosity	0.47
Bulk ignition temperature	310.8 K
Initial bed temperature	305.25 K
Bed length	200 mm
Disk rupture	14.3 MN/m^2 (2045 psi)
Total igniter (tetryl) mass	38.2 g
Typical mass of propellant in bed	99 g
Length of igniter discharge	12.5 mm

One way to retain some significant amount of mass entering the bed, and yet predict peak pressures that agree with the experiments is to increase the time which the initiator functions, thereby decreasing the discharge rate ψ.

After some additional cases for other combinations of ψ, it was decided that the best representation of the experiments with our one-dimensional model was to assume ψ = 1783.5 kg/m s^{-1}, and let t_p equal the time until disc rupture, giving a typical mass of M = 12.3 g, since $t_p = t_{dr}$ = 505 μs. This, of course, means that 25.90 g of the detonator charge was liberated after disk rupture or outside the bed, which is about what would be expected if the detonated pellet formed a spherical blast and only that section of the surface with the one-inch diameter opening entered the bed. The pressure history at the same four locations in the bed is shown as the dotted lines in Fig. 4 for these values. These pressure histories more closely reflect the peak pressure data of [4].

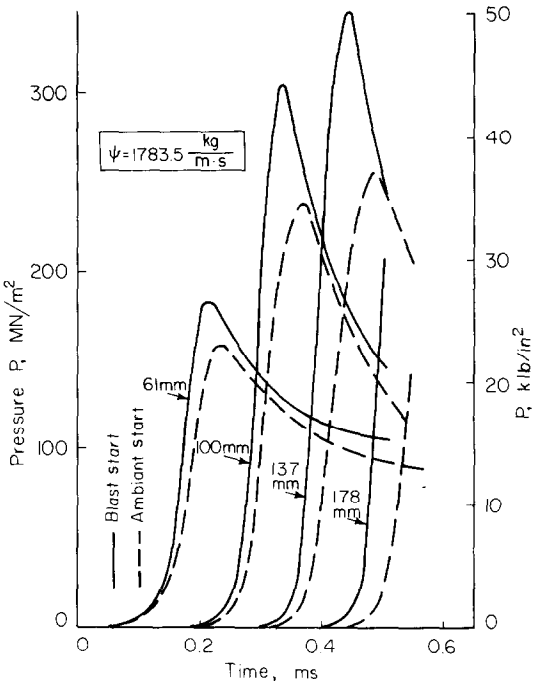

FIG. 4. Predicted pressure histories at the fair gage locations for a source strength assumed to represent the test conditions.

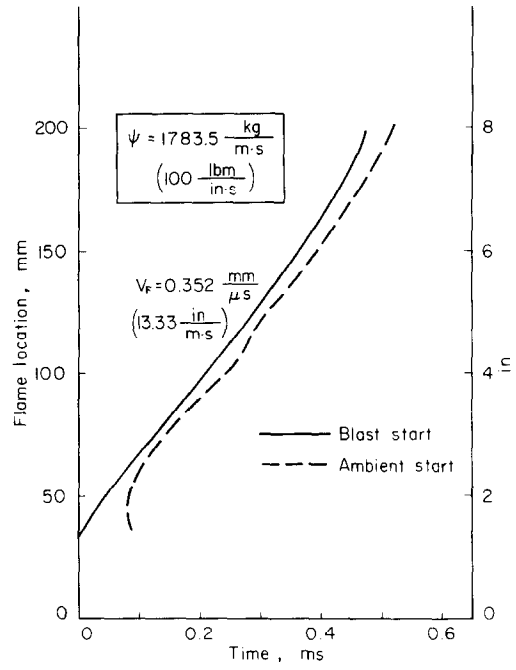

FIG. 6. Flame front locus for both blast start and ambient start conditions.

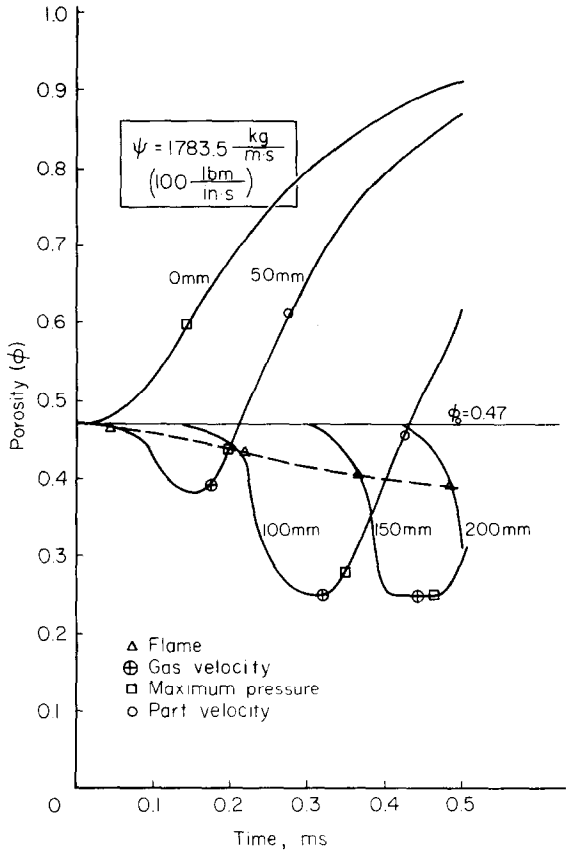

FIG. 5. Porosity history at four locations, indicating loci of flame front, maximum gas pressure and maximum particle velocity.

The solid lines represent a calculation in which the pressure at the first 25 mm igniter was exponential decreasing from 70 MPa to 0.1 MPa at time $t = 0$. The purpose here was to blast start the sequence of ignition. In order to maintain static equilibrium at time $t = 0$, the porosity must be variable to maintain this initial pressure gradient. As expected and shown in Fig. 4, this type of simulation results in greater peak pressures, but the pressure wave propagation and flame front are not greatly altered when compared to the ambient start. The predicted maximum gas velocity at the 100 mm location for the standard case of $\psi = 1784$ was 370 m/s and the maximum particle velocity was 265 m/s.

Figure 5 depicts the porosity history at four different locations, showing that, in the interior of the bed, one first observes a compaction (reduced ϕ) and then bed expansion. Part of this is due to the fact that the propellant has been ignited and is therefore loosing solid mass, and hence volume. Also indicated on this figure are the instant at those locations when the flame front arrives, and when the maximum pressure and velocities occur. Note that as one proceeds deeper into the bed that these "fronts" coalesce.

The flame location history is shown in Fig. 6 indicating that for this case the average flame velocity (which is the slope of the X_f vs t plot) was 0.352 mm/μs. The propellant ignition criterion was simply that the solid phase has been raised in temperature to the point where a critical energy of ignition has been deposited to the propellant [1].

Comparisons of the predicted maximum pressure with test results for actual M-30 propellant are shown in Fig. 7. Several different mass discharge conditions

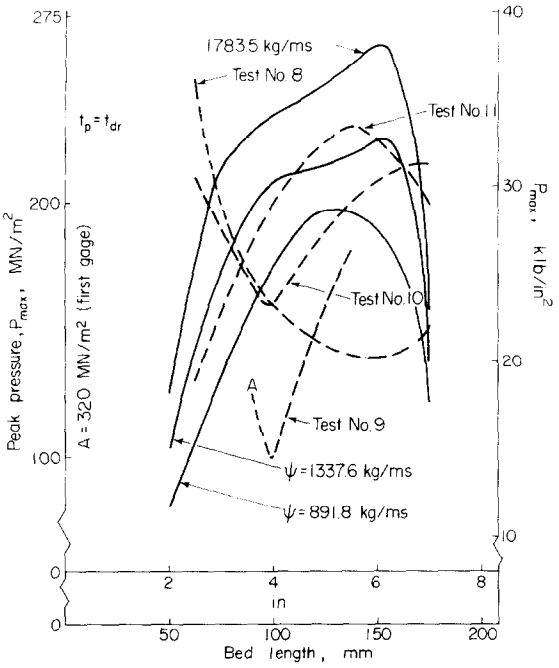

FIG. 7. Comparison of the peak pressure distribution predicted to those observed in the BRL experiments.

were compared on those figures. From peak pressure comparisons one might conclude that the one-dimensional flamespreading code used in this study simulates the bulk phenomena occurring in these packed beds which have been vigorously ignited. However, for some tests the peak pressure at the first gage location was much greater than the observed peak pressure at the interior gage positions. The model does not predict this at all, indicating to us that additional analysis will be required to adequately describe the blast ignition sequence.

Figure 8 (at two positions in the bed) shows that there is very little difference in the predicted pressure history for an *inert* bed, of the same size and loading

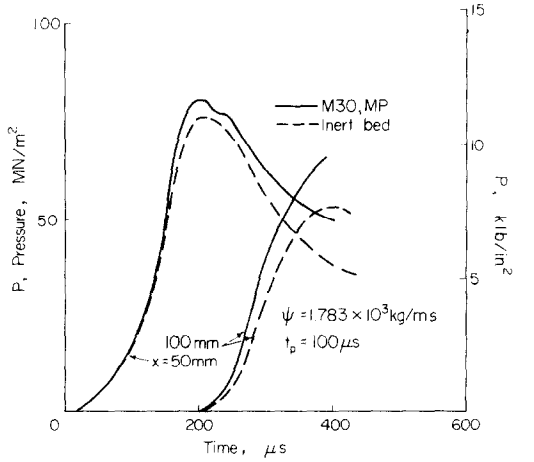

FIG. 8. Comparison of the predicted pressure history until disk rupture for flow in an inert bed to a bed a propellant.

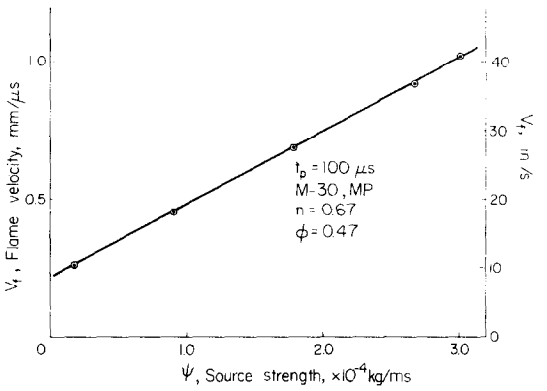

FIG. 9. Convective flame front speed for a range of sizeable ignitor mass source strength.

as a propellant bed. In the simulations for the inert bed (dotted lines on Fig. 8) the burning rate coefficients were simply set to zero. Notice with the condition of a very vigorous ignition source, the pressure wave propagation is basically determined by the strength of the initiator.

Wave propagation discussion

The pressure wave from the vigorous igniter propagates into the bed at a typical speed of 320 m/s. Here the pressure wave front is defined as the time at every location in which the pressure rises abruptly. For example, in Fig. 4 this is said to occur at 140 μs at $x = 61$ mm, at 267 μs at $x = 100$ mm, at 375 μs at 137 mm, and so on, giving an average speed of 0.320 mm/μs. This wave is preceeded by the flame front which propagates at a rate close to this value. Figure 9, however, shows the remarkable result that the flame front is a linear function of the source strength, ψ, i.e. the vigour of the igniter. In fact, for our configuration (l_p and t_p) one can write from Fig. 9 that the flame front velocity, V_f, in mm/μs can be expressed as

$$V_f = 0.215 + \frac{0.027 \cdot \psi}{1000} \qquad (18)$$

for $1500 < \psi < 30\,000$ kg/m·s and the mass distributed within 1.25 cm. Therefore, as increasing mass discharge provides for larger pressure and temperature gradients, as well as greater initial bed compaction, there results larger potential to drive the wave fronts.

The predicted disk rupture time as a function of source strength is shown in Fig. 10. It appears that a limiting asymptotic disk rupture time (at $x = 200$ mm) is being approached as the source strength becomes extremely large.

The computer code was set to read out a pressure gradient, dp/dx at every location at every time calculation. Figure 11 presents these values for the *negative* pressure-gradient history at four different locations in the bed for the standard case. Between 61 and 100 mm the time between peak negative pressure gradient is 138 μs, corresponding to a "compression" wave speed of 0.278 mm/μs.

Finally, to conclude the predictions, Fig. 12 presents the locus of points for the flame front, the pressure wave front, the arrival of a 70 MPa pressure magnitude, and the maximum negative pressure gradient magnitude. It is evident that the slope of these loci are all very nearly equal, suggesting a regular pattern to the wave dynamics in a bed vigorously ignited at one end. There does not appear to be a coalescing of the pressure wave front and the flame front, a condition that has suggested to Bernecker and Price [8] which would lead to a deflagration-to-detonation transition (DDT).

CONCLUDING REMARKS

After a total evaluation of the comparison of the theoretical predictions to the limited but informative experiments, the results lead to the following conclusions:

1. Vigorous ignition, that is, dumping hot exploded gases into a propellant bed, within durations of the order of 100 μs results in extreme pressures in the bed interior. Experiments with the configuration depicted in Fig. 1 have observed pressures in excess of 310 MPa (45 000 psia).

2. The one-dimensional code predicts pressures in order of magnitude greater than those observed, *if* one assumes that all of the mass of the detonated initiator enters the packed propellant bed. But fairly good predictions (when compared to the tests) for the peak pressure distribution result if one assumes that only a fraction of the blast, typically a third of the mass, enters the bed. Actually, if the detonated initiator results in a truly spherical blast, then only a maximum of approximately a third of the mass can enter the tube since the opening of the carriage is less than the diameter of the pellet.

3. It is obvious that the model can be evaluated as to its correctness, only if additional experimental data can be had. For example, information such as blast duration, flame front history, disk rupture time, and guarantee that the tube did not expand radially during the ignition sequence can be compared to the theoretical predictions.

4. With the vigorous initiation, the pressure history at the gage locations is predicted to be mainly due to the blast gases themselves. That is, before disk rupture, the predictions of the code for an inert propellant bed are often close to those of the actual propellant of the same geometry and loading. The experiments of [4] seem to indicate that this is true.

5. The code predicts that typically less than 30% of the propellant has been consumed before disk rupture. In certain experiments, the recovered propellant was weighed and it was reported that 31–46% was consumed [4].

6. The flame front and the subsequent pressure wave front is predicted to be a strong function of the initiator mass discharge rate. Therefore, conclusions as to the potential hazard of blast initiation of an ammunition box, from experiments with only one initiation strength, must be carefully considered. That is, if a detonating blast dumps in mass such as considered in the calcu-

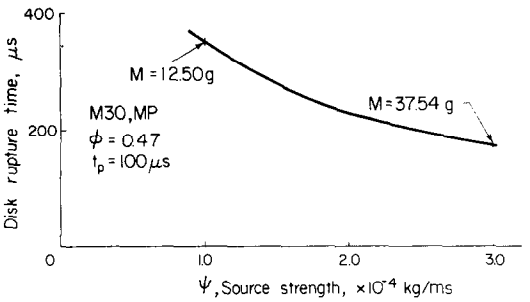

FIG. 10. Predicted disk rupture time as a function of ignitor source strength.

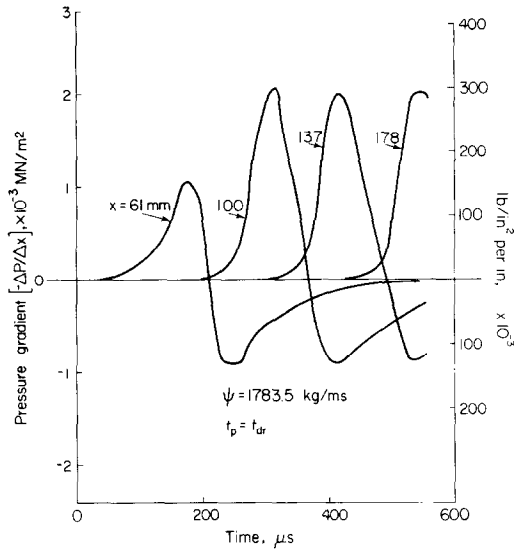

FIG. 11. Predicted time variation of the (negative) pressure gradient at the four gage locations, until disk rupture time ($\psi = 1784$).

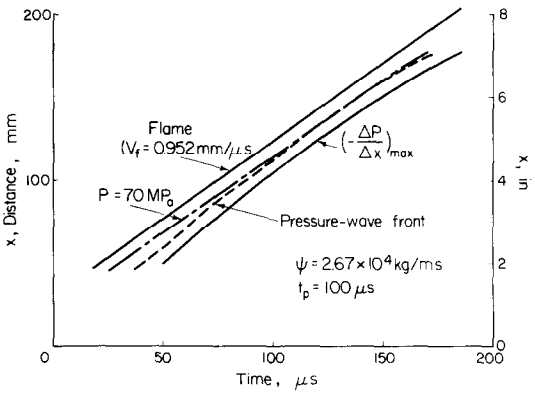

FIG. 12. Pressure wave propagation and flame front loci in a 20 cm long bed of M-30 propellant [ψ = 26.7 g/mm ms^{-1}].

lations shown in Fig. 2, the code predicts pressures in the excess of 250000 psia (1750 MPa). It is recommended that if more tests are to be performed in the same configuration, that different masses of the tetryl initiator be considered to confirm this concern.

7. The results shown in Fig. 12 indicate that the packed propellant bed will *not* itself detonate. The DDT mechanism concept of Bernecker and Price [7] were used to arrive at this conclusion. Only if considerable grain fracture from the initiation blast can produce propellant particles of much smaller size (and greater compaction) might there be appropriate conditions for detonating the bed. It is recommended that additional calculations be carried out with the code to study this possible hazard.

REFERENCES

1. H. Krier, W. F. Van Tassell and S. Rajan, Model of flame spreading and combustion through packed beds of propellant grains, Ballistic Research Contract Report BRL-CR-147 (March 1974).
2. W. F. Van Tassell and H. Krier, Combustion and flame spreading phenomena in gas-permeable explosive materials, *Int. J. Heat Mass Transfer* **18**(12), 1377–1386 (1975).
3. H. Krier, Predictions of flame spreading and pressure wave propagation in propellant beds, AAE Report No. 75-6, Aeronautical and Astronautical Engineering Department, University of Illinois at Urbana–Champaign (July 1975).
4. J. D. Knapton, I. C. Stobie and R. H. Comer, Vigorous ignition of M-30 propellant, Ballistic Research Interim Memorandum Report BRL IMR 320 and IMR 397 Interior Ballistic Lab, BRL, APG, Md. (December 1974; June 1975).
5. H. Krier and S. Gokhale, Vigorous ignition of granulated propellant beds by blast impact, AAE Report No. 75-7, Aeronautical and Astronautical Engineering Department, University of Illinois at Urbana–Champaign (August 1975).
6. S. L. Soo, *Fluid Dynamics of Multiphase Systems*. Blaisdell, Waltham, MA (1967).
7. S. L. Soo, Comments on mechanism of particle collision in one dimension dynamics of gas particle mixtures, *Physics Fluids* **8**(9), 1751–1752 (1965).
8. R. R. Bernecker and D. Price, Studies in the transition from deflagration to detonation in granular explosives, *Combust. Flame* Parts I, II, **22**, 111–129 (1974); Part III, **22**, 161–170 (1974).

APPENDIX

Typical Computer Printout Page

Z (in)	P (psi)	DP/DX (psi/in)	Gas vel. (in/s)	Part. vel. (in/s)	ϕ Porosity	Gas density (lb_m/in^3)	Gas temp. (deg R)	Part. temp. (deg R)
0.0	17337.0	0.0	0.0	0.0	0.793	0.268D-02	8035.0	495.0
0.200	17304.0	−2593.0	3045.3	939.96	0.792	0.269D-02	7977.2	497.1
0.400	17207.0	−6371.0	5982.5	1909.16	0.791	0.273D-02	7822.8	501.6
0.600	16986.0	−11100.0	8720.0	2905.95	0.787	0.277D-02	7601.6	507.6
0.800	16652.0	−13839.0	11178.0	3908.85	0.782	0.281D-02	7326.9	514.4
1.000	16294.0	−13937.0	13208.5	4889.05	0.773	0.288D-02	6996.7	521.5
1.200	15955.0	−12472.0	14768.2	5816.88	0.760	0.297D-02	6612.5	528.3
1.400	15670.0	−9488.0	15868.5	6664.50	0.742	0.311D-02	6171.6	560.0
1.600	15481.0	−4277.0	16476.3	7405.57	0.717	0.333D-02	5668.6	560.0
1.800	15456.0	4583.0	16544.1	8013.74	0.683	0.365D-02	5100.1	560.0
2.000	15710.0	20183.0	16171.6	8463.46	0.641	0.415D-02	4494.3	560.0
2.200	16465.0	40763.0	15302.0	8746.49	0.589	0.489D-02	3906.9	560.0
2.400	17748.0	66917.0	14322.4	8865.35	0.529	0.586D-02	3402.9	560.0
2.600	19811.0	93574.0	13316.3	8850.51	0.465	0.703D-02	3039.4	562.0
2.800	22427.0	112218.0	12304.3	8741.07	0.400	0.831D-02	2782.1	561.7
3.000	25422.0	135572.0	11649.3	8563.31	0.339	0.963D-02	2590.7	560.0
3.200	29205.0	134415.0	11458.6	8328.55	0.289	0.110D-01	2454.8	560.0
3.400	32143.0	26992.0	11775.8	8001.30	0.257	0.124D-01	2281.8	560.0
3.600	30555.0	−123139.0	12707.9	7471.67	0.250	0.129D-01	2030.9	560.0
3.800	25986.0	−239310.0	12688.5	6679.26	0.250	0.131D-01	1682.3	561.4
4.000	18590.0	−297748.0	12412.8	5493.21	0.250	0.128D-01	1253.4	566.0
4.200	11099.0	−266923.0	10875.5	4117.69	0.250	0.115D-01	875.9	568.9
4.400	5243.0	−180804.0	8845.1	2779.40	0.265	0.899D-02	586.8	569.0
4.600	2058.0	−87937.0	6991.0	1708.68	0.309	0.579D-02	400.1	566.5
4.800	847.0	−33405.0	5513.5	983.22	0.357	0.346D-02	296.7	562.6
5.000	388.0	−12684.0	4515.3	544.39	0.397	0.202D-02	243.6	558.9
5.200	212.0	−5170.0	3951.9	296.84	0.426	0.118D-02	234.3	555.9
5.400	130.0	−2567.0	3674.5	161.97	0.444	0.695D-03	245.5	553.8
5.600	84.0	−1450.0	3561.4	89.14	0.455	0.420D-03	265.4	552.4
5.800	57.0	−869.0	3478.9	49.57	0.461	0.263D-03	289.6	551.5
6.000	41.0	−533.0	3346.0	27.77	0.465	0.171D-03	316.6	550.9
6.200	30.0	−329.0	3123.1	15.60	0.467	0.118D-03	345.5	550.6
6.400	24.0	−203.0	2799.4	8.74	0.468	0.862D-04	375.3	550.4
6.600	20.0	−124.0	2391.3	4.85	0.469	0.672D-04	404.7	550.2
6.800	18.0	−75.0	1938.2	2.65	0.470	0.557D-04	432.2	550.1

APPENDIX

Typical Computer Printout Page

Z (in)	P (psi)	DP/DX (psi/in)	Gas vel. (in/s)	Part.vel. (in/s)	ϕ Porosity	Gas density (lb_m/in^3)	Gas temp. (deg R)	Part. temp. (deg R)
7.000	17.0	−44.0	1488.0	1.42	0.470	0.486D-04	456.9	550.1
7.200	16.0	−26.0	1079.4	0.74	0.470	0.442D-04	477.8	550.1
7.400	15.0	−15.0	732.7	0.37	0.470	0.414D-04	494.6	550.0
7.600	15.0	−8.0	448.4	0.17	0.470	0.398D-04	506.7	550.0
7.800	15.0	−3.0	211.9	0.07	0.470	0.389D-04	514.1	550.0
8.000	15.0	0.0	0.0	0.0	0.470	0.386D-04	516.5	550.0

Time: 0.31274D-03 s.
Position of leading edge: 8.0 in.
Velocity of leading edge: 0.0 in/s.
Wall temperature: 579.983 deg R.
Number of steps: 680, delta t, 0.49194D-06 s.

PREVISION DE LA DYNAMIQUE D'IGNITION BRUTALE D'UN LIT DE PARTICULES DE COMBUSTIBLE SOLIDE

Résumé—Cette étude contient les résultats fondamentaux d'un plan de recherche destiné à prévoir la propagation de l'onde de pression et le développement de la flamme dans une charge de combustible de propulsion, poreux et allumé à l'une de ses extrémités par un détonateur explosif. Les prévisions effectuées s'attachent à décrire les tests controlés en laboratoire réalisés avec de gros grains de combustible M30 confinés dans un cylindre et allumés par la détonation d'un disque explosif à son extrémité libre. On a trouvé que la valeur de la vitesse de décharge massique du détonateur détermine la vitesse du front de flamme convectif et l'onde de pression se propageant dans le lit de combustible.

BESTIMMUNG DER ZÜNDDYNAMIK EINES TREIBMITTELFESTBETTS

Zusammenfassung—In dieser Arbeit werden die wichtigsten Ergebnisse einer Untersuchung wiedergegeben, die Ausbreitung der Druckwellen und der Flammen in einer porösen Treibmittelladung zu bestimmen, die an einem Ende durch eine hochexplosive Initialzündung gezündet wurde. Die kontrollierten Laborversuche mit großkörnigem M30-Treibmittel, das in einem Zylinder eingeschlossen und durch eine Explosionsscheibe am offenen Ende gezündet wurde, sind modellmäßig dargestellt. Es zeigte sich, daß die Größe des Initialzündungs-Massenausstoßes die Geschwindigkeit der konvektiven Flammenfront und der sich ausbreitenden Druckwelle im Treibmittelbett bestimmt.

РАСЧЁТЫ ДИНАМИКИ ИНТЕНСИВНОГО ВОСПЛАМЕНЕНИЯ СЛОЯ ТВЁРДОГО РАКЕТНОГО ТОПЛИВА

Аннотация — Представлены основные результаты по расчету движения волны сжатия и распространения пламени в пористом заряде ракетного топлива, воспламеняемого с одного конца с помощью сильного детонатора. Расчёты проверялись лабораторными исследованиями с крупнозернистым ракетным топливом М-30, воспламеняемым путем детонации дисковым взрывателем у открытого конца. Показано, что интенсивность расхода массы воспламенителя определяет скорость конвективного фронта пламени и волну сжатия, распространяющуюся в слое топлива.